A "Nonlinear" Pursuit of Understanding Pollutant Accumulation and Chemistry at Environmental and Biological Interfaces

Andrew P. Carpenter[1,*], Thaddeus W. Golbek[2]

[1]School of Chemical, Biological, and Environmental Engineering, Oregon State University, Corvallis, Oregon, 97331

[2]Department of Chemistry, Aarhus University, 8000 Aarhus C, Denmark

*Author to whom correspondence should be addressed: carpeand@oregonstate.edu

Abstract

Over the past decade, public recognition of the prevalence of certain classes of pollutants, such as PFAS and nanoplastics, within the environment has sparked growing concerns over their potential impact on environmental and human health. Within both environmental and biological systems, the adsorption and structural organization of pollutants at aqueous interfaces can greatly impact the chemical reactivity and transformation. Experimentally probing chemical behavior at interfaces can often pose a problem due to bulk solvated molecules convoluting molecular signatures from interfacial molecules. To solve this problem there exist interface-*specific* nonlinear spectroscopy techniques that can directly probe both macroscopic planar interfaces and nanoplastic interfaces in aqueous environments. These techniques can provide essential information such as chemical adsorption, structure, and reactivity at interfaces. In this perspective, these techniques are presented with obvious advantages for studying the chemical properties of pollutants adsorbed to environmental and biological interfaces.

Introduction

At present, public anxieties are rising over nanoplastics (diameter < 1 μm) and perfluoroalkyl substances (PFAS) given their alarming concentrations and pervasiveness within the environment.[1-6] These compounds belong to a larger list of pollutants (*ex.* polycyclic aromatic hydrocarbons – PAH, polychlorinated biphenyls – PCB, pharmaceuticals, etc.) and understanding the impact of their presence in our environment is an urgent task.[7] In response to concerns over adverse health effects by exposure to pollutants, significant attention has been directed towards understanding the fate and transport of pollutants through the environment and the associated risks of exposure to humans and other hosts. Due to the amphiphilic nature of many pollutants it should be expected that they will accumulate at environmental interfaces, for example PFAS adsorbing to the air-foam interface.[8] Other types of interfaces found within our environment include water (air-water, mineral-water, etc.), aerosol, emulsion, and nanoplastic interfaces.[9-11] Accumulation of PFAS at the air-water interface within the aqueous thin films of foams near highly contaminated sites provides an important illustration of how pollutants accumulate at environmental interfaces in ways that have important health implications. At one site it was found that PFAS concentrations were enriched by over 1000 fold in the foam.[12] This translates into increased exposure risks for humans as the foam collects at the shoreline. Thus, it is critical to develop a fundamental understanding of pollutants at all interfaces, as molecular structure and activity can drastically change as pollutants adsorb to aqueous interfaces, compared to bulk properties.[13, 14] Furthermore, for nano-scale material pollutants, such as nanoplastics, the formation of the bio-corona at the nanoparticle interface defines the identity of the nano-material in the environment.[4, 15]

Environmental interfaces, however, aren't the only surfaces that should be considered in the study of interfacial chemistry of pollutants. Once a host (human or ecological) is exposed to pollutants, the interaction that occurs at the pollutant nanoparticle or membrane interface becomes

important. Understanding how PFAS incorporate into the lipid bilayers of various tissues, how eco- and bio-coronas around nanoplastics alter their membrane interactions and transport through the body, and whether certain pollutants are capable of crossing tissue barriers are all examples of important health related questions rooted in the interfacial chemistry of pollutants at membrane surfaces.

But how does one measure reaction kinetics at aqueous surfaces, determine molecular structure, and/or measure the adsorption of pollutants to complex and often buried interfaces? When does curvature and size of a nanomaterials, whether they be particles, emulsion, or lipid vesicles, begin to influence pollutant adsorption and chemistry? Embedded in these questions, and others, is a need to isolate the molecular interactions of interfacial bound pollutants from that of unbound pollutants.

The present challenge for common experimental techniques is lack of either a chemical specificity or an interface *specificity*. The latter experimental feature is distinguished from interface-*sensitivity* because to be interface sensitive, as opposed to specific, still allows for a convolution of experimental signatures of both "near interfacial" and interfacial chemicals. An example of this characteristic would be the sea-surface microlayer (SML).[16] SML sampling methods need to be interfacially sensitive (*ex.* rotating drums or glass plates),[17] but the physical region these methods probe will be much deeper than the first few molecular layers that form the interfacial region. Experimentally probing the chemistry of pollutants at nanoparticle or vesicle surfaces becomes even more challenging due to the buried nature of these interfaces. Current methods of directly probing molecules at extended planar or nanoparticle surfaces include Fourier transform infrared spectroscopy, circular dichroism spectroscopy, two-dimensional infrared (2D-IR) spectroscopy, and intrinsic/extrinsic fluorescence.[18, 19] However, these methods do not

discriminate between molecules at the interface and those unbound in solution. In addition, these methods will not be able to resolve molecular structure or orientation at the interface.

To overcome these challenges, second-order nonlinear spectroscopies offer an inherently interface sensitive approach to probe the chemistry of pollutants adsorbed to environmental and biological interfaces. Second-order nonlinear spectroscopies are surface-*specific* methods that can be built to detect the chemical signatures of pollutants adsorbed to extended planar interfaces or the surface of nanoparticles dispersed in a solvent. In this perspective we present the two most common methods, vibrational sum-frequency generation (VSFG) and second-harmonic generation (SHG), and consider how these techniques could be used to study the chemical behavior of pollutants adsorbed to environmental and biological interfaces.

Surface-Specific Nonlinear Optical Spectroscopies

Vibrational sum-frequency generation and second-harmonic generation spectroscopies are two interface-*specific* methods capable of detecting changes in the composition and molecular structure at interfaces.[20] VSFG measures the vibrational spectrum of adsorbed pollutants and ordered water at interfaces,[21] while SHG measurements are sensitive to ordered interfacial solvents or the presence of adsorbed chromophores in its non-resonant[22, 23] and resonant[24, 25] variations, respectively. While other optical spectroscopies, such as infrared reflection adsorption spectroscopy (IRRAS), are considered interface-sensitive, the interface-*specificity* of VSFG and SHG comes from the selection rule that any chemical environment must be asymmetrically ordered to generate a VSFG or SHG signal. Two illustrations of the difference between interface specificity versus sensitivity can be found in the ability of VSFG, but not infrared spectroscopy, to detect unbound water oscillators in the topmost layer of water at an aqueous interface or the surface-most

layer of polymer thin films.[26-28] Thus, the use of these spectroscopies to study pollutants directly at aqueous interfaces is a straightforward extension of previous applications.

VSFG and SHG techniques are collectively known as second-order nonlinear spectroscopies. The theory underlying second-order spectroscopic methods has been well established, with both mathematically rigorous[29, 30] and introductory[21, 31] descriptions available. Herein, we describe the information accessible by both spectroscopic methods and provide examples of model environmental and biological interfaces before turning to consider how these methods can be applied to study the interfacial chemical behavior of pollutants.

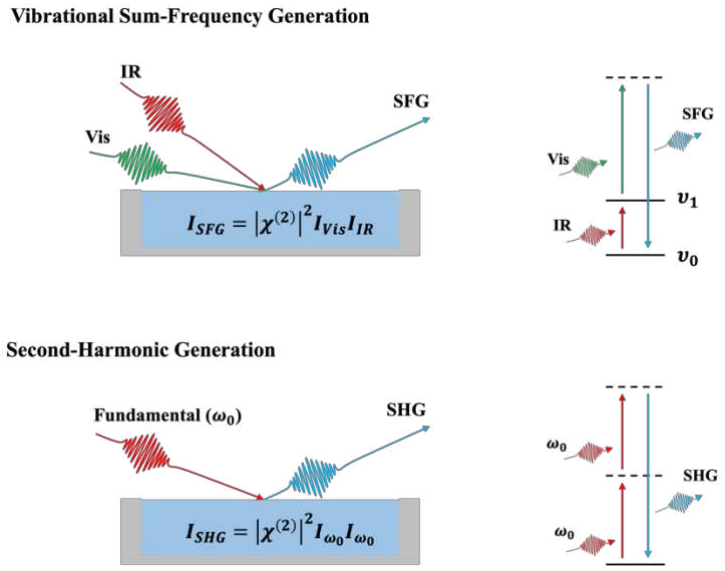

Figure 1. Illustration of experimental geometries (left) and Jablonski diagrams (right) for vibrational sum-frequency generation (VSFG) and second-harmonic generation (SHG). Inset in both illustrations is the general equation for the intensity of each second-order nonlinear process.

In the typical VSFG experiment, the sum-frequency response is generated from an aqueous interface by overlapping a mid-IR pulse and a fixed frequency visible pulse at the interface (Figure 1, top).[32-34] The mid-IR pulse frequency will vary between 1000-4000 cm^{-1}, with the pulse bandwidth dependent on the experimental system used in the VSFG study. The intensity of the sum-frequency response is dependent on the intensity of the incident infrared and visible laser

pulses, as well as the second-order surface susceptibility ($\chi^{(2)}$). The second-order susceptibility ($\chi^{(2)} \propto N\langle\beta^{(2)}\rangle$) includes contributions from the surface concentration (N) and average orientation of the molecular hyperpolarizability ($\langle\beta^{(2)}\rangle$) being measured.[21, 29] For a vibrational mode to appear in a sum-frequency spectrum it must be IR and Raman active and the molecule must have a net orientation (*i.e.* not isotropically distributed).[21] Therefore, a VSFG spectrum contains information pertaining to the molecular surface density, the local chemical environment, and molecular structure and orientation. For a comprehensive introduction to VSFG, a tutorial series has recently been assembled that approaches both the experimental and theoretical aspects of this technique.[31, 35-42]

SHG is governed by similar principles as VSFG, except the two incident excitation pulses are degenerate (Figure 1, bottom). In a SHG experiment, a single pulsed laser is incident on the interfaces and the intensity of the second harmonic of the incident beam is detected. Similar to VSFG experiments, the intensity of the second-harmonic response is dependent on the second-order susceptibility and the intensity of the incident beam. However, the composition of the second-order susceptibility will change depending on whether the two incident pulses in an SHG experiment are resonant[24, 25] or non-resonant[22] with an electronic excitation at the surface. For the resonant SHG case, where the energy of the two incident pulses is sufficient to excite an electronic dipole, the experiment is sensitive to the orientational ordering of whichever chromophore (*e.x.* malachite green) is adsorbed to the surface. In the non-resonant SHG case, where the energy of the two incident pulses is less than that required to excite an electronic dipole, the SHG experiment becomes a probe of the orientational ordering of interfacial water and interfacial electric fields.[22, 23, 43-47] It is noted that these solvent contributions will negligible in the resonant SHG condition due to the resonant enhancement of the electronic excitation being the dominant SHG response.

While VSFG and SHG experiments are commonly used to probe planar interfaces, the techniques have progressed and enabled researchers to study the interface of micro- and nano-particle dispersions. First demonstrated in the 1990's,[48, 49] second-harmonic scattering (SHS) spectroscopy in both the resonant[49] and non-resonant[44, 50] conditions has emerged as a powerful probe to understand molecular adsorption and the electric double layer at particle interfaces. A few years later, in 2003,[51] vibrational sum-frequency scattering (SFS) was first demonstrated leading to the experimental capability to measure vibrational spectra of nanoemulsion[52, 53] vesicle,[54] and water droplet[55, 56] interfaces. Collectively, SHG and VSFG, and their scattering counterparts, provide the essential interface-*specificity* experimental capabilities and have the potential to prove invaluable to understanding the pollution chemistry at environmental and biological interfaces.

Model Environmental Interfaces

Interface-specific nonlinear spectroscopies are already being applied to study some environmentally relevant interfaces. For instance, the air-water interface has historically been used as a model for aerosol interfaces. Here, VSFG has been used to study the reaction between CO_2 and monoethanolamine (a benchmark scrubber)[57], the hydration states and interfacial behavior of secondary organic aerosol precursors,[58, 59] changes in the protonation state of fatty acids,[60] and have observed the enhanced reaction rates of phenol radicals.[14] At the oil-water interface, a model interface used for oil spills, SHS and SFS studies have revealed the impact of interfacial electric fields on surfactant adsorption to nanoemulsion surfaces[61, 62] and provided insight into the stabilization of oil droplets by a component of the oil dispersant Corexit.[53, 63] VSFG and SHG have also been used to examine ion driven surface adsorption of carboxyl-containing polymers as a model for humic acid[64, 65] and investigate the surface pH of aqueous-oil interfaces.[66] Lastly,

nonlinear spectroscopic studies of metal oxide nanoparticles have helped provide insight into the hydration state and interfacial electric fields at their surfaces.[67, 68]

Model Biomimetic Interfaces

Models of biological membrane surfaces have also been studied using interface-*specific* spectroscopies. Lipid monolayers at the air-water interface and supported lipid bilayers at the solid-water interface have been the most common membrane models for surface-specific nonlinear spectroscopy.[51, 69-73] Golbek et al. used lipid monolayers as membrane models to show the antimicrobial peptide WLBU2 adopts a ß-sheet structure at mammalian membranes but an α-helix at bacterial membranes, providing molecular insight into its antimicrobial activity.[74] Engstrom et al. studied the interaction between silver nanoparticles and lipid monolayers, resulting in a mechanistic model to explain size-dependent nanoparticle toxicity.[75] Conboy and coworkers found supported lipid bilayers to be invaluable models to measure the lipid flip-flop rates using VSFG.[76, 77] These are but a few of the many VSFG and SHG studies at these planar membrane models.

Recent advances with nonlinear scattering spectroscopies SHS and SFS open new possibilities with the use of lipid vesicles and lipid stabilized nanoemulsions as 3D membrane models.[54, 78-80] For instance, at the nanoemulsion interface it was found LK-peptides orient in an upright fashion at the particle surface, as opposed to a flat orientation at the extended planar surface.[81] Protein-lipid binding studies are now possible, exemplified by the use of SFS to study lysozyme-lipid binding where it was shown the protein inserts itself into the lipid surface causing a conformational change in the lipid acyl chains and a reorientation of the lipid headgroups.[82] Using a vesicle model, Dedic et al. demonstrated SHS can detect α-synuclein binding the vesicle surface through changes in interfacial water ordering.[83]

Monitoring PFAS Adsorption at Environmental Interfaces

As the Environmental Protection Agency (USA) tightens limits on PFAS concentrations in drinking water (0.02 PPT),[84] opportunities arise to understand PFAS adsorption at environmental interfaces. Much of what is known about PFAS adsorption has been determined from laboratory experiments of fluorinated surfactants where control can be exerted over the ionic strength and dissolved organic matter concentrations. From well controlled laboratory experiments it is known that PFAS bulk properties and surface activity will differ relative to similar hydrogenated surfactants. PFAS micelle formation will be impacted by elevated Krafft temperature (minimum temperature required for micelle formation), resulting in changes in solubility and micelle formation.[85, 86] The fluorinated alkyl chains also results in PFAS saturating aqueous interfaces at lower bulk concentrations and a reduced CMC.[86, 87] At environmental interfaces, where the composition of the aqueous sub-phase is not controlled, measuring adsorption becomes more difficult. One method of measuring PFAS concentrations near environmental interfaces, within the SML,[88] uses glass plates to collect PFAS near the interface.[16] The PFAS content on these slides is then rinsed off, collected, and concentrations measured using analytical methods.[17] However, this method is not surface specific and will collect PFAS that reside below the top-most molecular layers that constitute the interface. Thus, to experimentally measuring PFAS surface behavior at environmental interfaces requires methods to detect PFAS chemical signatures with a surface-specificity.

One challenge in using traditional adsorption experiments, such as tensiometry, to determine molecular properties at liquid interfaces is the non-specific nature of these experiments. If the subphase contains unknown ion composition or unknown surface-active organics, any analysis of surface tensiometry results will be complicated by their presence. The C-F vibrational

modes of PFAS species provides vibrational resonances that are often isolated from other resonant modes and thus opens avenues to study their adsorption behavior at natural aqueous surfaces. Interestingly, published VSFG spectra of the C-F stretching region (~1250-1450 cm^{-1}) are rare, with fluorinated polymers being the focus of the majority of previous studies.[89-91] Some published works have used VSFG to monitor adsorption and calculate molecular orientation of perfluorononionic acid (PFNA) and fluorinated myristic acid at the air-water interface,[33, 92, 93] and it was recently demonstrated that VSFG spectra of the C-F stretching region can be used to estimate surface concentrations of PFAS adsorbed to river water-air interface.[94]

We have recently recorded VSFG spectra of a model PFAS (polyfluorinated dodecylphosphonic acid, F_{21}-DDPA) at the air-water interface of river water (Willamette River, Oregon, USA). In order to apply VSFG to measure adsorption isotherms, spectral contributions from changes in both molecular orientation and surface concentration need to be accounted for. Calculations of the molecular orientation from VSFG data have previously shown the average molecular orientation of fluorinated surfactant, including F_{21}-DDPA, is invariant to changes in surface density.[33, 94] Thus, it is can be assumed that orientation does not change and that the sum-frequency amplitude ($|E_{VSFG}| = \sqrt{I_{VSFG}}$) will be linearly related to PFAS interfacial density.[21] VSFG spectra of the F_{21}-DDPA C-F stretching vibrational modes were recorded in the PPP polarization combination at the river water-air interface (Willamette River, pH 7.5). We observe a linear relationship between PFAS surface density and sum-frequency amplitude (Figure 2). Details of the VSFG spectrometer used in these experiments can be found in elsewhere.[94] At this pH, F_{21}-DDPA is insoluble in the river water. Therefore, the surface concentration of F_{21}-DDPA was directly adjusted by dissolving in $CHCl_3$ and adding the solution dropwise to the neutral river water surface. After each addition, the C-F stretching spectrum was recorded (Figure 2a). From these

spectra the electric field amplitude was calculated from the spectral fits, revealing linear relationship between sum-frequency amplitude and the known surface density (Figure 2b).

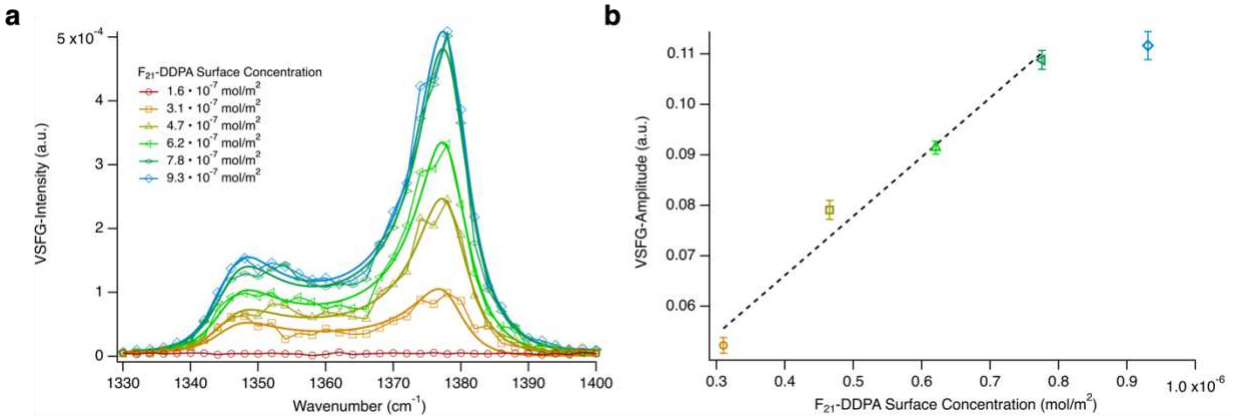

Figure 2. (a) VSFG spectra of F_{21}-DDPA adsorbed to the surface of Willamette River water – air interface (pH ~ 7.5). Spectra were recorded in the PPP polarization combination. Solid lines are spectra fits based on standard VSFG fitting (b) VSFG amplitudes for the vibrational mode at 1378 cm^{-1}, determined from spectral fits, plotted as a function of surface concentration. Linear dashed line is provided as a visual guide to the linear rise in VSFG amplitude.

Combining these VSFG spectra of PFAS at the river-water interface with recently published work,[94] it is clear that VSFG has potential to probe changes in PFAS surface concentrations at complex aqueous interfaces. However, work is needed to better understand the C-F vibrational region using VSFG and to push the detection limit towards environmentally relevant concentrations. For instance, it might be expected the SSP polarization combination would yield higher signal intensities than PPP and, therefore, be better suited for detecting low concentrations of PFAS. However, we have found spectral response for this vibrational region is stronger the PPP polarization combination, consistent with previous VSFG studies involving this spectral region.[33, 92] Future work is needed to model the C-F spectral response, which will aid in moving it towards a better probe of environmentally relevant concentrations. This is necessary as the bulk concentrations of the data shown here, and from previous work, are at least an order of magnitude higher than the concentrations found in the most contaminated waters.[95, 96] Future

application of VSFG to measure environmentally relevant concentrations should aim to detect interfacial PFAS at bulk concentrations of 1 μg/L or lower. VSFG methods exist that have a lower detection limit (e.g. heterodyne VSFG and electronic SFG),[97-100] and could possibly be utilized to pursue adsorption studies at concentrations relevant to PFAS river contamination sites.

Probing Pharmaceutical Adsorption to Nanoplastic Surfaces

The capacity of pollutants to adsorb to nanoparticle surfaces, causing the nanoparticle to become a reservoir for pollutants, is a phenomena currently being investigated.[101, 102] Adsorption of pollutants to nanoplastic surfaces can impact fate and transport of the nanoparticles and there are concerns over how pollutants adsorbed to the nanoplastics alter the toxicity of both the nanoplastic or pollutant.[101, 103-106] Yet, understanding pollutant adsorption at nanoparticle surfaces requires direct probing of the particle surface, which is extremely challenging as the particle surface is buried and distributed throughout a bulk medium. Adsorption studies to extended planar surfaces can produce relevant results for understanding adsorption at larger microplastic (>10 μm) surfaces, but adsorption to charged nanoplastic surfaces can't be accurately modeled by studies of planar interfaces due to interfacial electric fields suppressing adsorption[61, 62] and altering the interfacial structure of adsorbed materials.[52, 107]

Nonlinear scattering techniques, such as SHS and SFS, can directly probe nanoparticle surfaces and thus could provide critical insight into pollutant adsorption to nanoparticle surfaces. SFS has measured surfactant adsorption to the nanoemulsion surface.[52, 63, 81] Resonant SHS has been used to malachite green adsorption to nanoparticle surfaces[49] and non-resonant SHS has helped understand electric field effects on surfactant adsorption to nanoemulsion surfaces.[62]

Therefore, these experimental methods have potential to significantly contribute in our understanding of the interaction of pollutants at nanoparticle interfaces.

Here we illustrate how non-resonant SHS could be used to detect pollutant adsorption at environmentally relevant concentrations (Figure 3). Non-resonant SHS signal, for these experiments, is generated from ordered water molecules at the nanoparticle surface.[108] As such, the SHS signal will contain contributions from the ordered water dipole and interfacial electric fields through the higher-order $\chi^{(3)}$ tensor.[22, 109] These effects have been well documented and have been reviewed elsewhere.[108, 110, 111] As a proof of principle, we used non-resonant SHS to detect the adsorption of acetaminophen to polystyrene nanoparticles (PS-NP). Details of the SHS system for these experiments have been recently published.[112] Without acetaminophen PS-NP particles generate a SHS scattering pattern typical of 500 nm PS-NP particles (black trace, Figure 3b).[113] At 10 ng/L acetaminophen, SHS signal intensity is observed to increase slightly (red trace, Figure 3b) and even more at 1 μg/L acetaminophen (green trace, Figure 3b). The observed increase in SHS intensity is a direct consequence of acetaminophen adsorption to the PS-NP surfaces. Further experiments are required to untangle whether pollutant adsorption causes a change in the SHS signal through a shift in the interfacial electric fields or a reorientation of water dipoles, but perturbations to either could prove useful in the future as a probe of pollutant adsorption to nanoparticle surfaces. Notably, the concentrations probed here are on the same order of magnitude as pharmaceutical pollution found in wastewater and untreated drinking water.[114, 115] If SHS were combined with SFS, adsorption isotherms could be measured to determine free energies of adsorption, maximum surface coverage, and the concentrations of pollutants at nanoparticle surfaces.

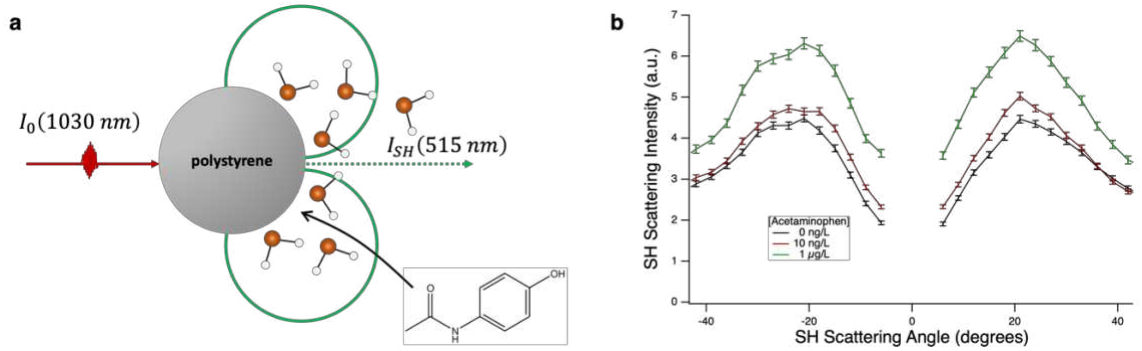

Figure 3. (a) Illustration of non-resonant SHS generation, experimental geometry, and the ordered water dipoles that give rise to non-resonant SHS signal. (b) SHS scattering patterns measured from PS-NP (500 nm diameter) in the absence (black trace) and presence of acetaminophen (red trace - 10 ng/L, green trace 1 µg/L). Measurements were made in the PP polarization combination. Error bars represent the relative standard error.

Nanoplastic Interactions with Biological Membranes

While questions over whether micro- and nanoplastics can be pollution reservoirs, these particles will become a potential health problem when humans are exposed to the pollutant coated particles. Nanoparticle toxicity is known to vary with the particle's physical properties (*i.e.* size, corona, charge, etc.),[15, 75, 116, 117] yet the molecular mechanism resulting in particle toxicity is a topic of ongoing investigation. When a nanoparticle enters the body, its fate can be influenced by interactions between the particle surface and biological tissue. Coating of the nanoparticle surface by organic or biological mass (eco- and bio-coronas) and the composition of the cellular membrane can all have an effect on nanoparticle interaction and subsequent nanoparticle uptake. Therefore, to develop an understanding of the molecular mechanism of nanoplastic toxicity and how it varies when the surface is modified, it will be necessary to study how nanoparticles interact with membrane interfaces.

At biomimetic membranes, VSFG has been used to discern structural perturbations to membrane structure as a result of nanoparticle adsorption.[75, 118, 119] By observing vibrational signatures associated with lipid acyl chains and headgroup, the average structural organization of

lipids within the model membrane can be determined and monitored under varying chemical conditions. At model cell membranes, the influence of surface coating and particle size/shape on lipid membrane structure have been studied for Au nanoparticles.[75, 119] Some of these observations were accompanied by toxicology studies, enabling VSFG to provide a mechanistic explanation for size dependent nanoparticle toxicity.[75] A similar approach can be used to observe nanoplastic interactions with biological membranes and reveal how membrane surfaces respond to adsorbed nanoplastics.

Mammalian cell membrane composition consists of nearly 50% phosphatidylcholine containing lipids.[120] Thus, a monolayer of DPPC (1,2-dipalmitoyl-sn-glycero-3-phosphocholine) was used as an initial model mammalian membrane. The lipid monolayer was formed by dropwise addition of a lipid solution to a water surface such that the final lipid density was 53 $Å^2$. VSFG spectra measurements of the DPPC monolayer in absence and presence of PS-NP (Figure 4) reveal lipid structure is changed in the presence of the nanoplastics. The C-D stretching region (2000 – 2300 cm^{-1}) probes the structural organization of the deuterated lipid acyl chains.[121] In the spectra shown here, the presence of PS-NP results in an increase in CD_3 intensity and loss of CD_2 intensity. This suggests the PS-NP have "snorkeled" through the monolayer,[122] compressing the lipids from a liquid expanded-liquid compressed phase into the liquid compressed phase.[51] Changes in the amplitude ratio between the CD_2 and CD_3 symmetric stretches have been used to discern changes in the conformational arrangement of lipid acyl chains.[74] Increase in the CD_3 symmetric stretch intensity and a decrease in the CD_2 symmetric stretch intensity indicate that the lipid acyl chains contain less gauche defects on average. This spectral change has been observed in VSFG measurements of changing lipid density[123] and has since been used to ascertain nanoparticle induced compression to biomimetic membrane surfaces.[75]

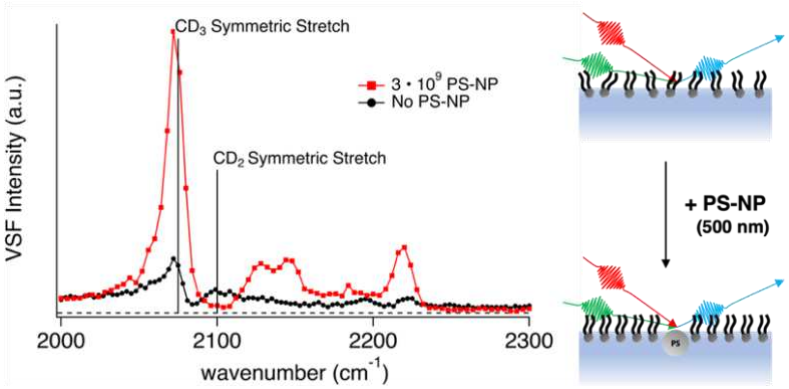

Figure 4. (left) VSFG spectra of a deuterated DPPC (53 Å^2/lipid) in the absence (black) and presence (red) of 500 nm PS-NP. The CD_3 and CD_2 peak centers are marked by the vertical solid lines. (right) Illustration of the VSFG experimental geometry and the compression of the lipid monolayer upon the addition of PS-NP.

Additional VSFG experiments could enable researchers to describe a more complete picture of the nanoplastic-lipid interaction. For instance, lipid vibrational groups such as the phosphate and carbonyl stretching vibrational modes can provide additional insight into the bonding interactions and hydration environment during nanoparticle-lipid interactions.[124-129] Further experiments could explore how modifications of nanoplastic surfaces, modeling different coronas, alter the particle-lipid interaction that could elucidate molecular mechanisms behind variations nanoplastic toxicity.[104, 117]

Future Prospects

This perspective has focused on illustrating the application of interface-specific nonlinear spectroscopies in the study of interfacial pollutant chemistry, with the experiments outlined here serving to demonstrate how these spectroscopic methods could be applied to the study of pollutant chemistry at environmental and biological interfaces. These examples have included measuring adsorption isotherms at complex aqueous interfaces, detecting pollutant adsorption to nanoparticle

surfaces, and discerning molecular structure and orientation within biomimetic membranes exposed to pollutants.

While these applications are promising, challenges exist that present technological hurdles to application and will be important to address. For instance, calculating molecular orientations relies on accurately measuring the second-order surface susceptibility. For nonlinear scattering experiments of nanoparticle surfaces, the incident beams pass through the bulk continuous phase where light absorption can distort the spectra. The process to correct spectra in absorptive media has already been demonstrated in water-oil systems,[130, 131] but will need to be expanded for complex aquatic matrices in order to determine molecular orientation at the surface of nanoplastics dispersed in natural aqueous media. Understanding the contributing vibrational modes in complex spectral regions will also have an impact on determining the structure of interfacial species. Resolving the interfacial orientation of PFAS from CF vibrational modes remains a challenge as computational modeling efforts have varied across studies, leading to inconsistencies in the calculated interfacial structures.[33, 92] Additional opportunities exist in ensuring spectrometer detection limits are capable of probing the interfacial behavior of environmentally and biologically relevant pollutant concentrations. Reliable model systems and experimental capabilities are being developed to better approximate the complex chemical environment of environmental and biological interfaces, which will provide solutions to these challenges.

It is worth noting that the illustrative experiments we have presented demonstrate none of the potential to observe chemical reactions at environmental interface. Since chemical and photochemical reactions will transform pollutants into new chemical species, it would be advantageous if the spectroscopic methods presented here could contribute to our understanding of these chemical transformations occurring within interfacial environments. To that end, recent

work has demonstrated there is much to be excited about with regards to the measurement of reaction kinetics at aqueous interfaces. Recent ultrafast VSFG measurements found the photochemical reaction of phenol becomes ultrafast at the air-water interface, with the reaction rate increasing ~10^4 times over the bulk reaction rate.[14] Subsequent theoretical work showed the enhanced reaction rates were the consequence the unique hydrogen bonding environment at the air-water interface stabilizing the excited electronic state, resulting in a reduced reaction barrier.[132] Since many persistent pollutants (*ex.* PAH and PCBs) contain aromatic structures, these studies could hint at an important role interfaces hold in the transformation of pollutants within the environment. The approach demonstrated by Kusaka et al. could provide an avenue to study how the hydrogen bonding environment of the aqueous interfaces impact the chemical reactivity and transformation of pollutants containing aromatic moieties.

Additional developments have recently successfully applied the suite of nonlinear scattering spectroscopies (SHS and SFS) to the study of liquid droplets, providing an avenue to *in situ* studies of aerosol interfaces. Some of the earliest studies demonstrated non-resonant SHS could be used to measure the second-harmonic scattering pattern from a water droplet surface and SFS could be used to measure vibrational spectra of an ethanol droplet surface.[133] Resonant SHS was then used to measure the adsorption of a dye to the surface of 100 nm aerosol surfaces, demonstrating aerosol surface were accessible with these techniques.[134] More recently, electronic and vibrational SFS have been used to measure electronic and vibrational spectra of molecules adsorbed to aerosol surfaces.[55, 135] Most intriguingly, when considering probing interfacial pollutant chemistry, vibrational SFS was used to measure adsorption isotherms of small organic molecules to the interface of 40 nm aerosols.[55] While there is an ongoing discussion as to how

aerosol particles of this size are capable of generating a measurable SFS signal,[55, 112, 136] these studies make it possible to envision future *in situ* studies of pollutant chemistry at aerosol surfaces.

Here we have described only some of the exciting possibilities of applying surface-specific nonlinear optical spectroscopy to the study of interfacial pollutant chemistry. With the past several decades of development laying the foundation, these methods are in the position to become powerful tools for probing pollutant chemistry within the unique chemical environments of environmental and biological interfaces.

Acknowledgements

APC would like to acknowledge support from the National Science Foundation Ascend Postdoctoral Research Fellowship under Grant 2137997. TWG thanks the Lundbeck Foundation for support of this work (postdoc grant R322-2019-2461). TWG acknowledge funding from the Novo Nordisk Foundation (New Exploratory Research and Discovery - NERD Grant, NNF22OC0074640). This article is part of a project that has received funding from the European Research Council (ERC) under the European Union's Horizon 2020 Research and Innovation Programme (Grant Agreement No. 819039 F-BioIce).

AUTHOR DECLARATIONS

Conflict of Interest

The authors have no conflicts to disclose.

Ethics Approval

No ethics approval was required for this work.

Data Availability

The data presented in this work are available upon request from the corresponding author.

References

(1) Pétré, M.-A.; Genereux, D. P.; Koropeckyj-Cox, L.; Knappe, D. R. U.; Duboscq, S.; Gilmore, T. E.; Hopkins, Z. R. Per- and Polyfluoroalkyl Substance (PFAS) Transport from Groundwater to Streams near a PFAS Manufacturing Facility in North Carolina, USA. *Environmental Science & Technology* **2021**, *55* (9), 5848-5856. DOI: 10.1021/acs.est.0c07978.

(2) Materić, D.; Peacock, M.; Dean, J.; Futter, M.; Maximov, T.; Moldan, F.; Röckmann, T.; Holzinger, R. Presence of nanoplastics in rural and remote surface waters. *Environmental Research Letters* **2022**, *17* (5), 054036. DOI: 10.1088/1748-9326/ac68f7.

(3) Kurwadkar, S.; Dane, J.; Kanel, S. R.; Nadagouda, M. N.; Cawdrey, R. W.; Ambade, B.; Struckhoff, G. C.; Wilkin, R. Per- and polyfluoroalkyl substances in water and wastewater: A critical review of their global occurrence and distribution. *Science of The Total Environment* **2022**, *809*, 151003. DOI: https://doi.org/10.1016/j.scitotenv.2021.151003.

(4) Lyu, X.; Xiao, F.; Shen, C.; Chen, J.; Park, C. M.; Sun, Y.; Flury, M.; Wang, D. Per- and Polyfluoroalkyl Substances (PFAS) in Subsurface Environments: Occurrence, Fate, Transport, and Research Prospect. *Reviews of Geophysics* **2022**, *60* (3), e2021RG000765, https://doi.org/10.1029/2021RG000765. DOI: https://doi.org/10.1029/2021RG000765 (acccessed 2023/03/03).

(5) Scearce, A. E.; Goossen, C. P.; Schattman, R. E.; Mallory, E. B.; MaCrae, J. D. Linking drivers of plant per- and polyfluoroalkyl substance (PFAS) uptake to agricultural land management decisions. *Biointerphases* **2023**, *18* (4), 040801. DOI: 10.1116/6.0002772 (acccessed 8/9/2023).

(6) Goossen, C. P.; Schattman, R. E.; MacRae, J. D. Evidence of compost contamination with per- and polyfluoroalkyl substances (PFAS) from "compostable" food serviceware. *Biointerphases* **2023**, *18* (3), 030501. DOI: 10.1116/6.0002746 (acccessed 8/9/2023).

(7) Lohmann, R.; Breivik, K.; Dachs, J.; Muir, D. Global fate of POPs: Current and future research directions. *Environmental Pollution* **2007**, *150* (1), 150-165. DOI: https://doi.org/10.1016/j.envpol.2007.06.051.

(8) Schwichtenberg, T.; Bogdan, D.; Carignan, C. C.; Reardon, P.; Rewerts, J.; Wanzek, T.; Field, J. A. PFAS and Dissolved Organic Carbon Enrichment in Surface Water Foams on a Northern U.S. Freshwater Lake. *Environmental Science & Technology* **2020**, *54* (22), 14455-14464. DOI: 10.1021/acs.est.0c05697.

(9) Wania, F.; Axelman, J.; Broman, D. A review of processes involved in the exchange of persistent organic pollutants across the air–sea interface. *Environmental Pollution* **1998**, *102* (1), 3-23. DOI: https://doi.org/10.1016/S0269-7491(98)00072-4.

(10) Cunliffe, M.; Engel, A.; Frka, S.; Gašparović, B.; Guitart, C.; Murrell, J. C.; Salter, M.; Stolle, C.; Upstill-Goddard, R.; Wurl, O. Sea surface microlayers: A unified physicochemical and biological perspective of the air–ocean interface. *Progress in Oceanography* **2013**, *109*, 104-116. DOI: https://doi.org/10.1016/j.pocean.2012.08.004.

(11) Yu, F.; Yang, C.; Zhu, Z.; Bai, X.; Ma, J. Adsorption behavior of organic pollutants and metals on micro/nanoplastics in the aquatic environment. *Science of The Total Environment* **2019**, *694*, 133643. DOI: https://doi.org/10.1016/j.scitotenv.2019.133643.

(12) Schaefer, C. E.; Lemes, M. C. S.; Schwichtenberg, T.; Field, J. A. Enrichment of poly- and perfluoroalkyl substances (PFAS) in the surface microlayer and foam in synthetic and

natural waters. *Journal of Hazardous Materials* **2022**, *440*, 129782. DOI: https://doi.org/10.1016/j.jhazmat.2022.129782.

(13) Wilson, K. R.; Prophet, A. M.; Rovelli, G.; Willis, M. D.; Rapf, R. J.; Jacobs, M. I. A kinetic description of how interfaces accelerate reactions in micro-compartments. *Chemical Science* **2020**, *11* (32), 8533-8545, 10.1039/D0SC03189E. DOI: 10.1039/D0SC03189E.

(14) Kusaka, R.; Nihonyanagi, S.; Tahara, T. The photochemical reaction of phenol becomes ultrafast at the air–water interface. *Nature Chemistry* **2021**, *13* (4), 306-311. DOI: 10.1038/s41557-020-00619-5.

(15) Cao, J.; Yang, Q.; Jiang, J.; Dalu, T.; Kadushkin, A.; Singh, J.; Fakhrullin, R.; Wang, F.; Cai, X.; Li, R. Coronas of micro/nano plastics: a key determinant in their risk assessments. *Particle and Fibre Toxicology* **2022**, *19* (1), 55. DOI: 10.1186/s12989-022-00492-9.

(16) Zhang, Z.; Liu, L.; Liu, C.; Cai, W. Studies on the sea surface microlayer: II. The layer of sudden change of physical and chemical properties. *Journal of Colloid and Interface Science* **2003**, *264* (1), 148-159. DOI: https://doi.org/10.1016/S0021-9797(03)00390-4.

(17) Schwichtenberg, T.; Bogdan, D.; Schaefer, C. E.; Stults, J.; Field, J. A. Per- and Polyfluoroalkyl Substances Enrichment in the Surface Microlayer of a Freshwater System Impacted by Aqueous Film-Forming Foams. *ACS ES&T Water* **2023**, *3* (4), 1150-1160. DOI: 10.1021/acsestwater.2c00618.

(18) zhang, M.; Fan, L.; Liu, Y.; Huang, S.; Li, J. Effects of proteins on emulsion stability: The role of proteins at the oil–water interface. *Food Chemistry* **2022**, *397*, 133726. DOI: https://doi.org/10.1016/j.foodchem.2022.133726.

(19) Chatterley, A. S.; Golbek, T. W.; Weidner, T. Measuring Protein Conformation at Aqueous Interfaces with 2D Infrared Spectroscopy of Emulsions. *The Journal of Physical Chemistry Letters* **2022**, *13* (31), 7191-7196. DOI: 10.1021/acs.jpclett.2c01324.

(20) Shen, Y. R. Surfaces probed by nonlinear optics. *Surface science* **1994**, *299-300*, 551-562, 10.1016/0039-6028(94)90681-5. DOI: papers3://publication/doi/10.1016/0039-6028(94)90681-5.

(21) Lambert, A. G.; Davies, P. B.; Neivandt, D. J. Implementing the Theory of Sum Frequency Generation Vibrational Spectroscopy: A Tutorial Review. *Applied Spectroscopy Reviews* **2005**, *40* (2), 103-145, 10.1081/ASR-200038326. DOI: papers3://publication/doi/10.1081/ASR-200038326.

(22) Ong, S.; Zhao, X.; Eisenthal, K. B. Polarization of water molecules at a charged interface: second harmonic studies of the silica/water interface. *Chemical Physics Letters* **1992**, *191* (3), 327-335. DOI: https://doi.org/10.1016/0009-2614(92)85309-X.

(23) Rehl, B.; Rashwan, M.; DeWalt-Kerian, E. L.; Jarisz, T. A.; Darlington, A. M.; Hore, D. K.; Gibbs, J. M. New Insights into χ(3) Measurements: Comparing Nonresonant Second Harmonic Generation and Resonant Sum Frequency Generation at the Silica/Aqueous Electrolyte Interface. *The Journal of Physical Chemistry C* **2019**, *123* (17), 10991-11000. DOI: 10.1021/acs.jpcc.9b01300.

(24) Hicks, J. M.; Kemnitz, K.; Eisenthal, K. B.; Heinz, T. F. Studies of liquid surfaces by second harmonic generation. *The Journal of Physical Chemistry* **1986**, *90* (4), 560-562. DOI: 10.1021/j100276a015.

(25) Eisenthal, K. B. Equilibrium and Dynamic Processes at Interfaces by Second Harmonic and Sum Frequency Generation. *Annual Review of Physical Chemistry* **1992**, *43* (1), 627-661. DOI: 10.1146/annurev.pc.43.100192.003211 (acccessed 2023/07/27).

(26) Du, Q.; Superfine, R.; Freysz, E.; Shen, Y. R. Vibrational spectroscopy of water at the vapor/water interface. **1993**, *70* (15), 2313-2316. DOI: 10.1103/physrevlett.70.2313.

(27) Chen, Z.; Ward, R.; Tian, Y.; Baldelli, S.; Opdahl, A.; Shen, Y.-R.; Somorjai, G. A. Detection of Hydrophobic End Groups on Polymer Surfaces by Sum-Frequency Generation Vibrational Spectroscopy. *Journal of the American Chemical Society* **2000**, *122* (43), 10615-10620. DOI: 10.1021/ja000808j.

(28) Gopalakrishnan, S.; Jungwirth, P.; Tobias, D. J.; Allen, H. C. Air−Liquid Interfaces of Aqueous Solutions Containing Ammonium and Sulfate: Spectroscopic and Molecular Dynamics Studies. *The Journal of Physical Chemistry B* **2005**, *109* (18), 8861-8872. DOI: 10.1021/jp0500236.

(29) Shen, Y.-R. *Fundamentals of Sum-Frequency Spectroscopy*; Cambridge University PRess, 2016.

(30) Morita, A. *Theory of Sum Frequency Spectroscopy*; Springer Singapore, 2018.

(31) Pickering, J. D.; Bregnhøj, M.; Chatterley, A. S.; Rasmussen, M. H.; Strunge, K.; Weidner, T. Tutorials in vibrational sum frequency generation spectroscopy. I. The foundations. *Biointerphases* **2022**, *17* (1), 011201. DOI: 10.1116/6.0001401 (acccessed 7/27/2023).

(32) Wang, J.; Even, M. A.; Chen, X.; Schmaier, A. H.; Waite, J. H.; Chen, Z. Detection of Amide I Signals of Interfacial Proteins in Situ Using SFG. *Journal of the American Chemical Society* **2003**, *125* (33), 9914-9915. DOI: 10.1021/ja036373s.

(33) Tyrode, E.; Johnson, C. M.; Rutland, M. W.; Day, J. P. R.; Bain, C. D. A Study of the Adsorption of Ammonium Perfluorononanoate at the Air−Liquid Interface by Vibrational Sum-Frequency Spectroscopy. *The Journal of Physical Chemistry C* **2007**, *111* (1), 316-329. DOI: 10.1021/jp063912h.

(34) Backus, E. H. G.; Bonn, D.; Cantin, S.; Roke, S.; Bonn, M. Laser-Heating-Induced Displacement of Surfactants on the Water Surface. *The Journal of Physical Chemistry B* **2012**, *116* (9), 2703-2712. DOI: 10.1021/jp2074545.

(35) Pickering, J. D.; Bregnhøj, M.; Chatterley, A. S.; Rasmussen, M. H.; Roeters, S. J.; Strunge, K.; Weidner, T. Tutorials in vibrational sum frequency generation spectroscopy. II. Designing a broadband vibrational sum frequency generation spectrometer. *Biointerphases* **2022**, *17* (1), 011202. DOI: 10.1116/6.0001403 (acccessed 2022/02/25).

(36) Carpenter, A. P.; Baio, J. E. Choose your own adventure: Picosecond or broadband vibrational sum-frequency generation spectroscopy. *Biointerphases* **2022**, *17* (3), 031201. DOI: 10.1116/6.0001844 (acccessed 7/30/2023).

(37) Doughty, B.; Lin, L.; Premadasa, U. I.; Ma, Y.-Z. Considerations in upconversion: A practical guide to sum-frequency generation spectrometer design and implementation. *Biointerphases* **2022**, *17* (2), 021201. DOI: 10.1116/6.0001817 (acccessed 7/27/2023).

(38) Chen, Z. Early sum frequency generation vibrational spectroscopic studies on peptides and proteins at interfaces. *Biointerphases* **2022**, *17* (3), 031202. DOI: 10.1116/6.0001859 (acccessed 8/9/2023).

(39) Hosseinpour, S. Dos and don'ts tutorial for sample alignment in sum frequency generation spectroscopy. *Biointerphases* **2022**, *17* (3), 031203. DOI: 10.1116/6.0001851 (acccessed 8/9/2023).

(40) Pickering, J. D.; Bregnhøj, M.; Rasmussen, M. H.; Strunge, K.; Weidner, T. Tutorials in vibrational sum frequency generation spectroscopy. III. Collecting, processing, and analyzing vibrational sum frequency generation spectra. *Biointerphases* **2022**, *17* (4), 041201. DOI: 10.1116/6.0001951 (acccessed 8/9/2023).

(41) Yang, L.; Zhang, W.; Bian, H.; Ma, G. Tutorial on the instrumentation of sum frequency generation vibrational spectroscopy: Using a Ti:sapphire based system as an example. *Biointerphases* **2022**, *17* (5), 051201. DOI: 10.1116/6.0002007 (acccessed 8/9/2023).

(42) Moloney, E. G.; Azam, M. S.; Cai, C.; Hore, D. K. Vibrational sum frequency spectroscopy of thin film interfaces. *Biointerphases* **2022**, *17* (5), 051202. DOI: 10.1116/6.0002085 (acccessed 8/9/2023).

(43) Goh, M. C.; Hicks, J. M.; Kemnitz, K.; Pinto, G. R.; Heinz, T. F.; Eisenthal, K. B.; Bhattacharyya, K. Absolute orientation of water molecules at the neat water surface. *The Journal of Physical Chemistry* **1988**, *92* (18), 5074-5075. DOI: 10.1021/j100329a003.

(44) Konek, C. T.; Musorrafiti, M. J.; Al-Abadleh, H. A.; Bertin, P. A.; Nguyen, S. T.; Geiger, F. M. Interfacial Acidities, Charge Densities, Potentials, and Energies of Carboxylic Acid-Functionalized Silica/Water Interfaces Determined by Second Harmonic Generation. *Journal of the American Chemical Society* **2004**, *126* (38), 11754-11755. DOI: 10.1021/ja0474300.

(45) Hayes, P. L.; Malin, J. N.; Jordan, D. S.; Geiger, F. M. Get charged up: Nonlinear optical voltammetry for quantifying the thermodynamics and electrostatics of metal cations at aqueous/oxide interfaces. *Chemical Physics Letters* **2010**, *499* (4), 183-192. DOI: https://doi.org/10.1016/j.cplett.2010.09.060.

(46) Roesel, D.; Eremchev, M.; Schönfeldová, T.; Lee, S.; Roke, S. Water as a contrast agent to quantify surface chemistry and physics using second harmonic scattering and imaging: A perspective. *Applied Physics Letters* **2022**, *120* (16), 160501. DOI: 10.1063/5.0085807 (acccessed 2022/09/20).

(47) Ray, K. K.; Limaye, A.; Ng, K. C.; Saha, A.; Shin, S.; Biswas, B.; Gaigeot, M.-P.; Pezzotti, S.; Willard, A. P.; Allen, H. C. Second-Harmonic Generation Provides Insight into the Screening Response of the Liquid Water Interface. *The Journal of Physical Chemistry C* **2023**. DOI: 10.1021/acs.jpcc.3c02605.

(48) Wang, H.; Yan, E. C. Y.; Borguet, E.; Eisenthal, K. B. Second harmonic generation from the surface of centrosymmetric particles in bulk solution. *Chemical Physics Letters* **1996**, *259* (1), 15-20. DOI: papers3://publication/uuid/25380A75-5ABD-45ED-8102-A56A91C89CE2.

(49) Wang, H.; Yan, E. C. Y.; Liu, Y.; Eisenthal, K. B. Energetics and Population of Molecules at Microscopic Liquid and Solid Surfaces. *The Journal of Physical Chemistry B* **1998**, *102* (23), 4446-4450. DOI: 10.1021/jp980491y.

(50) Roke, S.; Gonella, G. Nonlinear Light Scattering and Spectroscopy of Particles and Droplets in Liquids. *Annual Review of Physical Chemistry* **2012**, *63* (1), 353-378, 10.1146/annurev-physchem-032511-143748. DOI: papers3://publication/doi/10.1146/annurev-physchem-032511-143748.

(51) Roke, S.; Roeterdink, W. G.; Wijnhoven, J. E. G. J.; Petukhov, A. V.; Kleyn, A. W.; Bonn, M. Vibrational Sum Frequency Scattering from a Submicron Suspension. *Physical Review Letters* **2003**, *91* (25), 258302.

(52) de Aguiar, H. B.; Strader, M. L.; de Beer, A. G. F.; Roke, S. Surface Structure of Sodium Dodecyl Sulfate Surfactant and Oil at the Oil-in-Water Droplet Liquid/Liquid Interface: A Manifestation of a Nonequilibrium Surface State. *The Journal of Physical Chemistry B* **2011**, *115* (12), 2970-2978, 10.1021/jp200536k. DOI: papers3://publication/doi/10.1021/jp200536k.

(53) Hensel, J. K.; Carpenter, A. P.; Ciszewski, R. K.; Schabes, B. K.; Kittredge, C. T.; Moore, F. G.; Richmond, G. L. Molecular characterization of water and surfactant AOT at nanoemulsion surfaces. *Proceedings of the National Academy of Sciences* **2017**, *114* (51), 13351, 10.1073/pnas.1700099114.

(54) Strader, M. L.; de Aguiar, H. B.; de Beer, A. G. F.; Roke, S. Label-free spectroscopic detection of vesicles in water using vibrational sum frequency scattering. *Soft Matter* **2011**, *7* (10), 4959-4963, 10.1039/c0sm01358g. DOI: papers3://publication/doi/10.1039/c0sm01358g.

(55) Qian, Y.; Brown, J. B.; Huang-Fu, Z.-C.; Zhang, T.; Wang, H.; Wang, S.; Dadap, J. I.; Rao, Y. In situ analysis of the bulk and surface chemical compositions of organic aerosol particles. *Communications Chemistry* **2022**, *5* (1), 58. DOI: 10.1038/s42004-022-00674-8.

(56) Qian, Y.; Brown, J. B.; Zhang, T.; Huang-Fu, Z.-C.; Rao, Y. In Situ Detection of Chemical Compositions at Nanodroplet Surfaces and In-Nanodroplet Phases. *The Journal of Physical Chemistry A* **2022**, *126* (23), 3758-3764. DOI: 10.1021/acs.jpca.2c03346.

(57) McWilliams, L. E.; Valley, N. A.; Vincent, N. M.; Richmond, G. L. Interfacial Insights into a Carbon Capture System: CO2 Uptake to an Aqueous Monoethanolamine Surface. *The Journal of Physical Chemistry A* **2017**, *121* (41), 7956-7967. DOI: 10.1021/acs.jpca.7b07742.

(58) Wren, S. N.; Gordon, B. P.; Valley, N. A.; McWilliams, L. E.; Richmond, G. L. Hydration, Orientation, and Conformation of Methylglyoxal at the Air–Water Interface. *The Journal of Physical Chemistry A* **2015**, *119* (24), 6391-6403. DOI: 10.1021/acs.jpca.5b03555.

(59) Gordon, B. P.; Moore, F. G.; Scatena, L. F.; Richmond, G. L. On the Rise: Experimental and Computational Vibrational Sum Frequency Spectroscopy Studies of Pyruvic Acid and Its Surface-Active Oligomer Species at the Air–Water Interface. *The Journal of Physical Chemistry A* **2019**, *123* (49), 10609-10619. DOI: 10.1021/acs.jpca.9b08854.

(60) Tyrode, E.; Corkery, R. Charging of Carboxylic Acid Monolayers with Monovalent Ions at Low Ionic Strengths: Molecular Insight Revealed by Vibrational Sum Frequency Spectroscopy. *The Journal of Physical Chemistry C* **2018**, *122* (50), 28775-28786. DOI: 10.1021/acs.jpcc.8b09505.

(61) Zdrali, E.; Chen, Y.; Okur, H. I.; Wilkins, D. M.; Roke, S. The Molecular Mechanism of Nanodroplet Stability. *ACS Nano* **2017**, *11* (12), 12111-12120. DOI: 10.1021/acsnano.7b05100.

(62) Glikman, D.; Braunschweig, B. Nanoscale Effects on the Surfactant Adsorption and Interface Charging in Hexadecane/Water Emulsions. *ACS Nano* **2021**, *15* (12), 20136-20147. DOI: 10.1021/acsnano.1c08038.

(63) Carpenter, A. P.; Foster, M. J.; Jones, K. K.; Richmond, G. L. Effects of Salt-Induced Charge Screening on AOT Adsorption to the Planar and Nanoemulsion Oil–Water Interfaces. *Langmuir* **2021**, *37* (29), 8658-8666. DOI: 10.1021/acs.langmuir.0c03606.

(64) Robertson, E. J.; Beaman, D. K.; Richmond, G. L. Designated Drivers: The Differing Roles of Divalent Metal Ions in Surfactant Adsorption at the Oil–Water Interface. *Langmuir* **2013**, *29* (50), 15511-15520, 10.1021/la403665n. DOI: papers3://publication/doi/10.1021/la403665n.

(65) Robertson, E. J.; Carpenter, A. P.; Olson, C. M.; Ciszewski, R. K.; Richmond, G. L. Metal Ion Induced Adsorption and Ordering of Charged Macromolecules at the Aqueous/Hydrophobic Liquid Interface. *The Journal of Physical Chemistry C* **2014**, *118* (28), 15260-15273. DOI: 10.1021/jp503051w.

(66) Gan, W.; Wu, W.; Yang, F.; Hu, D.; Fang, H.; Lan, Z.; Yuan, Q. The behavior of hydroxide and hydronium ions at the hexadecane–water interface studied with second harmonic generation and zeta potential measurements. *Soft Matter* **2017**, *13* (43), 7962-7968, 10.1039/C7SM00813A. DOI: 10.1039/C7SM00813A.

(67) Bischoff, M.; Biriukov, D.; Předota, M.; Marchioro, A. Second Harmonic Scattering Reveals Ion-Specific Effects at the SiO2 and TiO2 Nanoparticle/Aqueous Interface. *The Journal of Physical Chemistry C* **2021**, *125* (45), 25261-25274. DOI: 10.1021/acs.jpcc.1c07191.

(68) Bischoff, M.; Kim, N. Y.; Joo, J. B.; Marchioro, A. Water Orientation at the Anatase TiO2 Nanoparticle Interface: A Probe of Surface pKa Values. *The Journal of Physical Chemistry Letters* **2022**, *13* (37), 8677-8683. DOI: 10.1021/acs.jpclett.2c02453.

(69) Bonn, M.; Roke, S.; Berg, O.; Juurlink; Stamouli, A.; Müller, M. A Molecular View of Cholesterol-Induced Condensation in a Lipid Monolayer. *The Journal of Physical Chemistry B* **2004**, *108* (50), 19083-19085. DOI: 10.1021/jp0452249.

(70) Zhang, C.; Myers, J. N.; Chen, Z. Elucidation of molecular structures at buried polymer interfaces and biological interfaces using sum frequency generation vibrational spectroscopy. *Soft Matter* **2013**, *9* (19), 4738-4761, 10.1039/C3SM27710K. DOI: 10.1039/C3SM27710K.

(71) Liu, W.; Wang, Z.; Fu, L.; Leblanc, R. M.; Yan, E. C. Y. Lipid Compositions Modulate Fluidity and Stability of Bilayers: Characterization by Surface Pressure and Sum Frequency Generation Spectroscopy. *Langmuir* **2013**, *29* (48), 15022-15031. DOI: 10.1021/la4036453.

(72) Bina, M.; Sciortino, F.; Mahrir, A. N. Phase separation in polymer-based biomimetic structures containing planar membranes. *Biointerphases* **2022**, *17* (6), 060802. DOI: 10.1116/6.0002078 (acccessed 8/9/2023).

(73) Ghosh, N.; Roy, S.; Mondal, J. A. Headgroup-Specific Interaction of Biological Lipid Monolayer/Water Interface with Perfluorinated Persistent Organic Pollutant (f-POP): As Observed with Interface-Selective Vibrational Spectroscopy. *The Journal of Physical Chemistry B* **2022**, *126* (2), 563-571. DOI: 10.1021/acs.jpcb.1c08214.

(74) Golbek, T. W.; Franz, J.; Elliott Fowler, J.; Schilke, K. F.; Weidner, T.; Baio, J. E. Identifying the selectivity of antimicrobial peptides to cell membranes by sum frequency generation spectroscopy. *Biointerphases* **2017**, *12* (2), 02D406. DOI: 10.1116/1.4982710 (acccessed 2020/12/23).

(75) Engstrom, A. M.; Faase, R. A.; Marquart, G. W.; Baio, J. E.; Mackiewicz, M. R.; Harper, S. L. Size-Dependent Interactions of Lipid-Coated Gold Nanoparticles: Developing a Better Mechanistic Understanding Through Model Cell Membranes and in vivo Toxicity. *International Journal of Nanomedicine* **2020**, *15*, 4091-4104. DOI: 10.2147/IJN.S249622.

(76) Liu, J.; Conboy, J. C. 1,2-Diacyl-Phosphatidylcholine Flip-Flop Measured Directly by Sum-Frequency Vibrational Spectroscopy. *Biophysical Journal* **2005**, *89* (4), 2522-2532. DOI: 10.1529/biophysj.105.065672 (acccessed 2023/08/04).

(77) Allhusen, J. S.; Conboy, J. C. The Ins and Outs of Lipid Flip-Flop. *Accounts of Chemical Research* **2017**, *50* (1), 58-65. DOI: 10.1021/acs.accounts.6b00435.

(78) Schmüser, L.; Golbek, T.; Weidner, T. Windowless detection geometry for sum frequency scattering spectroscopy in the C–D and amide I regions. *Biointerphases* **2021**, *16* (1), 011201-undefined. DOI: 10.1116/6.0000419.

(79) Okur, H. I.; Tarun, O. B.; Roke, S. Chemistry of Lipid Membranes from Models to Living Systems: A Perspective of Hydration, Surface Potential, Curvature, Confinement and Heterogeneity. *Journal of the American Chemical Society* **2019**, *141* (31), 12168-12181. DOI: 10.1021/jacs.9b02820.

(80) Chen, Y.; Jena, K. C.; Lütgebaucks, C.; Okur, H. I.; Roke, S. Three Dimensional Nano "Langmuir Trough" for Lipid Studies. *Nano Letters* **2015**, *15* (8), 5558-5563. DOI: 10.1021/acs.nanolett.5b02143.

(81) Golbek, T. W.; Strunge, K.; Chatterley, A. S.; Weidner, T. Peptide Orientation at Emulsion Nanointerfaces Dramatically Different from Flat Surfaces. *The Journal of Physical Chemistry Letters* **2022**, *13* (46), 10858-10862. DOI: 10.1021/acs.jpclett.2c02870.

(82) Golbek, T. W.; Okur, H. I.; Kulik, S.; Dedic, J.; Roke, S.; Weidner, T. Lysozyme Interaction with Phospholipid Nanodroplets Probed by Sum Frequency Scattering Vibrational Spectroscopy. *Langmuir* **2023**, *39* (18), 6447-6454. DOI: 10.1021/acs.langmuir.3c00276.

(83) Dedic, J.; Rocha, S.; Okur, H. I.; Wittung-Stafshede, P.; Roke, S. Membrane–Protein–Hydration Interaction of α-Synuclein with Anionic Vesicles Probed via Angle-Resolved Second-Harmonic Scattering. *The Journal of Physical Chemistry B* **2019**, *123* (5), 1044-1049. DOI: 10.1021/acs.jpcb.8b11096.

(84) *Drinking Water Health Advisories for PFOA and PFOS*. EPA, 2022. https://www.epa.gov/sdwa/drinking-water-health-advisories-pfoa-and-pfos (accessed 2023 February 06, 2023).

(85) Nakayama, H.; Shinoda, K. z. The Effect of Added Salts on the Solubilities and Krafft Points of Sodium Dodecyl Sulfate and Potassium Perfluoro-octanoate. *Bulletin of the Chemical Society of Japan* **1967**, *40* (8), 1797-1799. DOI: 10.1246/bcsj.40.1797 (acccessed 2023/06/20).

(86) Rosen, M. J. *Surfactants and Interfacial Phenomena*; Wiley-Interscience, 2004.

(87) Shinoda, K.; Hato, M.; Hayashi, T. Physicochemical properties of aqueous solutions of fluorinated surfactants. *The Journal of Physical Chemistry* **1972**, *76* (6), 909-914. DOI: 10.1021/j100650a021.

(88) Wurl, O.; Wurl, E.; Miller, L.; Johnson, K.; Vagle, S. Formation and global distribution of sea-surface microlayers. *Biogeosciences* **2011**, *8* (1), 121-135. DOI: 10.5194/bg-8-121-2011.

(89) Even, M. A.; Lee, S.-H.; Wang, J.; Chen, Z. Detection and Spectral Analysis of Trifluoromethyl Groups at a Surface by Sum Frequency Generation Vibrational Spectroscopy. *The Journal of Physical Chemistry B* **2006**, *110* (51), 26089-26097. DOI: 10.1021/jp065221r.

(90) Kristalyn, C. B.; Lu, X.; Weinman, C. J.; Ober, C. K.; Kramer, E. J.; Chen, Z. Surface Structures of an Amphiphilic Tri-Block Copolymer in Air and in Water Probed Using Sum Frequency Generation Vibrational Spectroscopy. *Langmuir* **2010**, *26* (13), 11337-11343. DOI: 10.1021/la100701b.

(91) Volpati, D.; Chachaj-Brekiesz, A.; Souza, A. L.; Rimoli, C. V.; Miranda, P. B.; Oliveira, O. N.; Dynarowicz-Łątka, P. Semifluorinated thiols in Langmuir monolayers – A study by nonlinear and linear vibrational spectroscopies. *Journal of Colloid and Interface Science* **2015**, *460*, 290-302. DOI: https://doi.org/10.1016/j.jcis.2015.08.069.

(92) Okuno, M.; Homma, O.; Kuo, A.-T.; Urata, S.; Koguchi, R.; Miyajima, T.; Ishibashi, T.-a. Molecular Orientations and Conformations of Air/Fluoroalkyl Acrylate Polymer Interfaces Studied by Heterodyne-Detected Vibrational Sum Frequency Generation. *Macromolecules* **2019**, *52* (22), 8705-8712. DOI: 10.1021/acs.macromol.9b00541.

(93) Nojima, Y.; Shimoaka, T.; Hasegawa, T.; Ishibashi, T.-a. Molecular Orientations of Myristic Acid Derivatives with Different Perfluoroalkyl Chain Lengths at the Air/Water Interface Evaluated by Heterodyne-Detected Sum Frequency Generation Spectroscopy. *The Journal of Physical Chemistry C* **2023**, *127* (25), 12349-12356. DOI: 10.1021/acs.jpcc.3c02636.

(94) Carpenter, A. P.; White, J. N.; Hasbrook, A.; Reierson, M.; Baio, J. E. Comparative Thermodynamic and Structural Analysis of Polyfluorinated Dodecylphosphonic Acid

Adsorption to Distilled and River Water Interfaces. *The Journal of Physical Chemistry A* **2023**, *127* (29), 6091-6099. DOI: 10.1021/acs.jpca.3c01487.

(95) Hale, S. E.; Arp, H. P. H.; Slinde, G. A.; Wade, E. J.; Bjørseth, K.; Breedveld, G. D.; Straith, B. F.; Moe, K. G.; Jartun, M.; Høisæter, Å. Sorbent amendment as a remediation strategy to reduce PFAS mobility and leaching in a contaminated sandy soil from a Norwegian firefighting training facility. *Chemosphere* **2017**, *171*, 9-18. DOI: https://doi.org/10.1016/j.chemosphere.2016.12.057.

(96) Høisæter, Å.; Pfaff, A.; Breedveld, G. D. Leaching and transport of PFAS from aqueous film-forming foam (AFFF) in the unsaturated soil at a firefighting training facility under cold climatic conditions. *Journal of Contaminant Hydrology* **2019**, *222*, 112-122. DOI: https://doi.org/10.1016/j.jconhyd.2019.02.010.

(97) Stiopkin, I. V.; Jayathilake, H. D.; Bordenyuk, A. N.; Benderskii, A. V. Heterodyne-Detected Vibrational Sum Frequency Generation Spectroscopy. *Journal of the American Chemical Society* **2008**, *130* (7), 2271-2275. DOI: 10.1021/ja076708w.

(98) Yamaguchi, S.; Otosu, T. Progress in phase-sensitive sum frequency generation spectroscopy. *Physical Chemistry Chemical Physics* **2021**, *23* (34), 18253-18267, 10.1039/D1CP01994E. DOI: 10.1039/D1CP01994E.

(99) Kumar, Y.; Dhami, S.; Pandey, R. Theoretical study of electronic sum frequency generation spectroscopy to assess the buried interfaces. *Biointerphases* **2023**, *18* (4), 041202. DOI: 10.1116/6.0002698 (acccessed 8/9/2023).

(100) Dhami, S.; Kumar, Y.; Pandey, R. Development of electronic sum frequency generation spectrophotometer to assess the buried interfaces. *Biointerphases* **2023**, *18* (4), 041201. DOI: 10.1116/6.0002697 (acccessed 8/9/2023).

(101) Liu, J.; Ma, Y.; Zhu, D.; Xia, T.; Qi, Y.; Yao, Y.; Guo, X.; Ji, R.; Chen, W. Polystyrene Nanoplastics-Enhanced Contaminant Transport: Role of Irreversible Adsorption in Glassy Polymeric Domain. *Environmental Science & Technology* **2018**, *52* (5), 2677-2685. DOI: 10.1021/acs.est.7b05211.

(102) Kiran, B. R.; Kopperi, H.; Venkata Mohan, S. Micro/nano-plastics occurrence, identification, risk analysis and mitigation: challenges and perspectives. *Reviews in Environmental Science and Bio/Technology* **2022**, *21* (1), 169-203. DOI: 10.1007/s11157-021-09609-6.

(103) Davranche, M.; Veclin, C.; Pierson-Wickmann, A.-C.; El Hadri, H.; Grassl, B.; Rowenczyk, L.; Dia, A.; Ter Halle, A.; Blancho, F.; Reynaud, S.; et al. Are nanoplastics able to bind significant amount of metals? The lead example. *Environmental Pollution* **2019**, *249*, 940-948. DOI: https://doi.org/10.1016/j.envpol.2019.03.087.

(104) Trevisan, R.; Uzochukwu, D.; Di Giulio, R. T. PAH Sorption to Nanoplastics and the Trojan Horse Effect as Drivers of Mitochondrial Toxicity and PAH Localization in Zebrafish. *Frontiers in Environmental Science* **2020**, *8*, Original Research. DOI: 10.3389/fenvs.2020.00078.

(105) Ramsperger, A. F. R. M.; Narayana, V. K. B.; Gross, W.; Mohanraj, J.; Thelakkat, M.; Greiner, A.; Schmalz, H.; Kress, H.; Laforsch, C. Environmental exposure enhances the internalization of microplastic particles into cells. *Science Advances* **2020**, *6* (50), eabd1211. DOI: 10.1126/sciadv.abd1211 (acccessed 2023/07/28).

(106) Gao, M.; Bai, L.; Li, X.; Wang, S.; Song, Z. Effects of polystyrene nanoplastics on lead toxicity in dandelion seedlings. *Environmental Pollution* **2022**, *306*, 119349. DOI: https://doi.org/10.1016/j.envpol.2022.119349.

(107) Zdrali, E.; Etienne, G.; Smolentsev, N.; Amstad, E.; Roke, S. The interfacial structure of nano- and micron-sized oil and water droplets stabilized with SDS and Span80. *The Journal of Chemical Physics* **2019**, *150* (20), 204704. DOI: 10.1063/1.5083844 (acccessed 2020/04/29).

(108) Gonella, G.; Dai, H.-L. Second Harmonic Light Scattering from the Surface of Colloidal Objects: Theory and Applications. *Langmuir* **2014**, *30* (10), 2588-2599, 10.1021/la403570f. DOI: papers3://publication/doi/10.1021/la403570f.

(109) Ohno, P. E.; Wang, H.-f.; Geiger, F. M. Second-order spectral lineshapes from charged interfaces. *Nature Communications* **2017**, *8* (1), 1032. DOI: 10.1038/s41467-017-01088-0.

(110) Geiger, F. M. Second Harmonic Generation, Sum Frequency Generation, and χ(3): Dissecting Environmental Interfaces with a Nonlinear Optical Swiss Army Knife. *Annual Review of Physical Chemistry* **2009**, *60* (1), 61-83. DOI: 10.1146/annurev.physchem.59.032607.093651 (acccessed 2020/05/02).

(111) Chu, B.; Marchioro, A.; Roke, S. Size dependence of second-harmonic scattering from nanoparticles: Disentangling surface and electrostatic contributions. *The Journal of Chemical Physics* **2023**, *158* (9), 094711. DOI: 10.1063/5.0135157 (acccessed 7/28/2023).

(112) Marchioro, A.; Golbek, T. W.; Chatterley, A. S.; Weidner, T.; Roke, S. A discrepancy of 107 in experimental and theoretical density detection limits of aerosol particles by surface

nonlinear light scattering. *Communications Chemistry* **2023**, *6* (1), 114. DOI: 10.1038/s42004-023-00903-8.

(113) Wunderlich, S.; Schürer, B.; Sauerbeck, C.; Peukert, W.; Peschel, U. Molecular Mie model for second harmonic generation and sum frequency generation. *Physical Review B* **2011**, *84* (23), 235403. DOI: 10.1103/PhysRevB.84.235403.

(114) Focazio, M. J.; Kolpin, D. W.; Barnes, K. K.; Furlong, E. T.; Meyer, M. T.; Zaugg, S. D.; Barber, L. B.; Thurman, M. E. A national reconnaissance for pharmaceuticals and other organic wastewater contaminants in the United States — II) Untreated drinking water sources. *Science of The Total Environment* **2008**, *402* (2), 201-216. DOI: https://doi.org/10.1016/j.scitotenv.2008.02.021.

(115) Zhang, P.; Zhou, H.; Li, K.; Zhao, X.; Liu, Q.; Li, D.; Zhao, G.; Wang, L. Occurrence of pharmaceuticals and personal care products, and their associated environmental risks in Guanting Reservoir and its upstream rivers in north China. *RSC Advances* **2018**, *8* (9), 4703-4712, 10.1039/C7RA12945A. DOI: 10.1039/C7RA12945A.

(116) Halimu, G.; Zhang, Q.; Liu, L.; Zhang, Z.; Wang, X.; Gu, W.; Zhang, B.; Dai, Y.; Zhang, H.; Zhang, C.; et al. Toxic effects of nanoplastics with different sizes and surface charges on epithelial-to-mesenchymal transition in A549 cells and the potential toxicological mechanism. *Journal of Hazardous Materials* **2022**, *430*, 128485. DOI: https://doi.org/10.1016/j.jhazmat.2022.128485.

(117) Li, L.; Li, S.; Xu, Y.; Ren, L.; Yang, L.; Liu, X.; Dai, Y.; Zhao, J.; Yue, T. Distinguishing the nanoplastic–cell membrane interface by polymer type and aging properties: translocation,

transformation and perturbation. *Environmental Science: Nano* **2023**, *10* (2), 440-453, 10.1039/D2EN00800A. DOI: 10.1039/D2EN00800A.

(118) Hu, P.; Zhang, X.; Li, Y.; Pichan, C.; Chen, Z. Molecular Interactions Between Silver Nanoparticles and Model Cell Membranes. *Topics in Catalysis* **2018**, *61* (9), 1148-1162. DOI: 10.1007/s11244-018-0926-1.

(119) Golbek, T. W.; Harper, B. J.; Harper, S. L.; Baio, J. E. Shape-dependent gold nanoparticle interactions with a model cell membrane. *Biointerphases* **2022**, *17* (6), 061003. DOI: 10.1116/6.0002183 (acccessed 7/28/2023).

(120) Henneberry, A. L.; Wright, M. M.; McMaster, C. R. The Major Sites of Cellular Phospholipid Synthesis and Molecular Determinants of Fatty Acid and Lipid Head Group Specificity. *Molecular Biology of the Cell* **2002**, *13* (9), 3148-3161. DOI: 10.1091/mbc.01-11-0540 (acccessed 2023/07/28).

(121) Tyrode, E.; Hedberg, J. A Comparative Study of the CD and CH Stretching Spectral Regions of Typical Surfactants Systems Using VSFS: Orientation Analysis of the Terminal CH3 and CD3 Groups. *The Journal of Physical Chemistry C* **2012**, *116* (1), 1080-1091. DOI: 10.1021/jp210013g.

(122) Van Lehn, R. C.; Atukorale, P. U.; Carney, R. P.; Yang, Y.-S.; Stellacci, F.; Irvine, D. J.; Alexander-Katz, A. Effect of Particle Diameter and Surface Composition on the Spontaneous Fusion of Monolayer-Protected Gold Nanoparticles with Lipid Bilayers. *Nano Letters* **2013**, *13* (9), 4060-4067. DOI: 10.1021/nl401365n.

(123) Guyot-Sionnest, P. H., J. H.; Shen, Y. R. Sum-Frequency Vibrational Spectroscopy of a Langmuir Film - Study of Molecular-Orientation of a Two-Dimensional System. *Phys. Rev. Lett.* **1987**, *59* (14), 1597-1600.

(124) Ma, G.; Allen, H. C. DPPC Langmuir Monolayer at the Air−Water Interface: Probing the Tail and Head Groups by Vibrational Sum Frequency Generation Spectroscopy. *Langmuir* **2006**, *22* (12), 5341-5349. DOI: 10.1021/la0535227.

(125) Chen, X.; Hua, W.; Huang, Z.; Allen, H. C. Interfacial Water Structure Associated with Phospholipid Membranes Studied by Phase-Sensitive Vibrational Sum Frequency Generation Spectroscopy. *Journal of the American Chemical Society* **2010**, *132* (32), 11336-11342. DOI: 10.1021/ja1048237.

(126) Bilkova, E.; Pleskot, R.; Rissanen, S.; Sun, S.; Czogalla, A.; Cwiklik, L.; Róg, T.; Vattulainen, I.; Cremer, P. S.; Jungwirth, P.; et al. Calcium Directly Regulates Phosphatidylinositol 4,5-Bisphosphate Headgroup Conformation and Recognition. *Journal of the American Chemical Society* **2017**, *139* (11), 4019-4024. DOI: 10.1021/jacs.6b11760.

(127) Dreier, L. B.; Bernhard, C.; Gonella, G.; Backus, E. H. G.; Bonn, M. Surface Potential of a Planar Charged Lipid–Water Interface. What Do Vibrating Plate Methods, Second Harmonic and Sum Frequency Measure? *The Journal of Physical Chemistry Letters* **2018**, *9* (19), 5685-5691. DOI: 10.1021/acs.jpclett.8b02093.

(128) Dreier, L. B.; Bonn, M.; Backus, E. H. G. Hydration and Orientation of Carbonyl Groups in Oppositely Charged Lipid Monolayers on Water. *The Journal of Physical Chemistry B* **2019**, *123* (5), 1085-1089. DOI: 10.1021/acs.jpcb.8b12297.

(129) Nojima, Y.; Yamaguchi, S. Heterodyne-Detected Sum Frequency Generation Spectroscopic Study of Weakly Hydrogen-Bonded Water at Charged Lipid Interfaces, Revisited. *The Journal of Physical Chemistry C* **2021**, *125* (42), 23483-23489. DOI: 10.1021/acs.jpcc.1c07173.

(130) Kulik, S.; Pullanchery, S.; Roke, S. Vibrational Sum Frequency Scattering in Absorptive Media: A Theoretical Case Study of Nano-objects in Water. *The Journal of Physical Chemistry C* **2020**, *124* (42), 23078-23085. DOI: 10.1021/acs.jpcc.0c05196.

(131) Carpenter, A. P.; Christoffersen, E. L.; Mapile, A. N.; Richmond, G. L. Assessing the Impact of Solvent Selection on Vibrational Sum-Frequency Scattering Spectroscopy Experiments. *The Journal of Physical Chemistry B* **2021**, *125* (12), 3216-3229. DOI: 10.1021/acs.jpcb.1c00188.

(132) Ishiyama, T.; Tahara, T.; Morita, A. Why the Photochemical Reaction of Phenol Becomes Ultrafast at the Air–Water Interface: The Effect of Surface Hydration. *Journal of the American Chemical Society* **2022**, *144* (14), 6321-6325. DOI: 10.1021/jacs.1c13336.

(133) Smolentsev, N.; Chen, Y.; Jena, K. C.; Brown, M. A.; Roke, S. Sum frequency and second harmonic generation from the surface of a liquid microjet. *The Journal of Chemical Physics* **2014**, *141* (18), 18C524. DOI: 10.1063/1.4896996 (acccessed 2020/04/30).

(134) Wu, Y.; Li, W.; Xu, B.; Li, X.; Wang, H.; McNeill, V. F.; Rao, Y.; Dai, H.-L. Observation of Organic Molecules at the Aerosol Surface. *The Journal of Physical Chemistry Letters* **2016**, *7* (12), 2294-2297. DOI: 10.1021/acs.jpclett.6b00872.

(135) Qian, Y.; Deng, G.-h.; Rao, Y. In Situ Spectroscopic Probing of Polarity and Molecular Configuration at Aerosol Particle Surfaces. *The Journal of Physical Chemistry Letters* **2020**, *11* (16), 6763-6771. DOI: 10.1021/acs.jpclett.0c02013.

(136) Qian, Y.; Brown, J. B.; Huang-Fu, Z.-C.; Zhang, T.; Wang, H.; Wang, S.; Dadap, J. I.; Rao, Y. Reply to: A discrepancy of 107 in experimental and theoretical density detection limits of aerosol particles by surface nonlinear light scattering. *Communications Chemistry* **2023**, *6* (1), 115. DOI: 10.1038/s42004-023-00904-7.